On Optimization of RIS-Assisted Secure UAV-NOMA Communications with Finite Blocklength

Dan ZHAO [1], Linzi HU [2], Wei XIONG [3], Huan CAI [2], Yuwen QIAN [2], Yutao XING [2]

[1] School of Electric and Optical Engineering, Nanjing University of Science and Technology ZiJin College, Nanjing, China
[2] School of Electric and Optical Engineering, Nanjing University of Science Technology, Nanjing, China
[3] Inner Mongolia Power (Group) Co., Ltd, Hohhot, China

admon@njust.edu.cn

Submitted May 15, 2024 / Accepted August 29, 2024 / Online first September 30, 2024

Abstract. *The combination of reconfigurable intelligent surface (RIS) with the unmanned aerial vehicle (UAV) and the non-orthogonal multiple access (NOMA) has emerged as a promising technology in the sixth generation (6G) network. However, UAV downlinks are susceptible to potential eavesdropping attacks due to the open and broadcasting nature of wireless channels. In addition, transmitting information with infinite blocklength (IBL) is impractical in 6G applications. In this paper, we propose a secure RIS-assisted UAV communication system based on NOMA with finite blocklength (FBL) transmission. To maximize the average secrecy rate for all ground users under the mobility and power constraints of the UAV, we jointly optimize the phase shift of the RIS, the trajectory, the transmit power of the UAV, and the user scheduling. To solve the formulated non-convex problem, we first transform the optimization problem into four convex sub-problems, i.e., phase shift optimization, trajectory optimization, transmit power optimization, and user scheduling optimization. Then, an iterative algorithm is developed based on the successive convex approximation (SCA) to solve the four sub-problems. Numerical results show that the average secrecy rate for all ground users achieved with the proposed algorithm is higher than that achieved with the traditional algorithms.*

Keywords

Information security, reconfigurable intelligent surface, unmanned aerial vehicle, NOMA, finite blocklength

1. Introduction

In recent years, unmanned aerial vehicles (UAVs) have been widely used in commercial and military applications due to their flexibility, cost-effectiveness, and application diversity [1], [2]. Especially, to satisfy the high quality of service (QoS) requirements under explosive data growth, the applications of UAVs with wireless communications have become an inevitable trend in the 5th generation (5G) and 6th generation (6G) network [3], [4]. On the one hand, UAVs can act as aerial relays or base stations (BSs) to improve coverage and capacity [5]. On the other hand, UAVs can be utilized as mobile terminals within cellular networks under special situations, such as entertainment, disaster relief, and military actions [6], [7]. However, since the open and broadcasting nature of wireless channels, UAV communication links are susceptible to potential eavesdropping attacks, leading to information leakage [8]. Moreover, due to the mobility and load limitation of UAVs, the security strategies in cryptography are not necessarily applicable to UAV-aided wireless networks [9].

Reconfigurable intelligent surface (RIS), which is composed of many low-cost passive reflective elements, has been recently proposed to solve the above physical layer security (PLS) problem [10], [11]. As a promising technology in the 6G network, RIS can reconfigure the wireless propagation environment and improve the quality of communications [12], [13]. The authors of [14] proposed a RIS-assisted directional modulation network, where each node is configured with multiple antennas. The secrecy rate was significantly enhanced with the assistance of RIS. However, reference [14] considered the scenario without the UAV. Moreover, in [15], a joint optimization algorithm was proposed to maximize the secrecy rate of the legitimate link in a single-user communication system aided by RIS. Furthermore, in [16], [17], multiple-user communication was considered and a RIS was utilized in the UAV networks to enhance communication security. However, there are few researches reported on the non-orthogonal multiple access (NOMA) techniques in RIS-assisted UAV networks.

Recently, the combination of the UAV and NOMA to cope with massive connectivity and high-speed transmission has received intensive attention [18]. NOMA has the advantages of high spectral efficiency, dense coverage, and high fairness [19]. The core idea of NOMA is to adopt superposition coding (SC) at the transmitters, and successive interference cancellation (SIC) at the receivers. For instance, reference [20] optimized the resource allocation,

DOI: 10.13164/re.2024.0526

the 3D trajectory design of the UAV, and the phase shift of the RIS jointly to minimize the average total power consumption in an IRS-assisted UAV-NOMA communication system. Furthermore, reference [21] investigated the RIS-enhanced multi-UAV NOMA networks to obtain the maximum sum rate of all users via jointly optimizing the 3D placement and transmit power of UAVs, the reflection matrix of the RIS, and the NOMA decoding orders. However, references [20], [21] ignored the impact of the RIS for PLS in the UAV-aided NOMA communication system.

Moreover, in multiple user communications, we often assume that the transmitted confidential information (CI) has infinite blocklength (IBL), which is unrealizable in practice [22]. In addition, to facilitate trajectory design, the flight period of the UAV is generally discretized into N time slots, with the duration of each time slot assumed to be sufficiently small to improve accuracy that can be significantly influenced by transmitting CI with IBL [23]. Furthermore, to support the new service type of ultra-reliable and low latency communications in 5G and 6G cellular systems, packet transmissions with finite blocklength (FBL) are widely used in various applications [24]. For example, reference [25] analyzed the system performance in a RIS-assisted UAV-IoT communication system with FBL codes. Even though much of the research has been focused on RIS-assisted UAV-NOMA networks, the PLS of RIS-assisted UAV-NOMA networks in the case of FBL transmission is still a challenging problem.

In this paper, we propose a novel secure RIS-assisted UAV-NOMA communication system, where a RIS is deployed to assist a UAV in transmitting CI with FBL to legitimate ground users in the presence of eavesdroppers. To maximize the average secrecy rate of all ground users, we propose an optimization algorithm by jointly optimizing the phase shift of the RIS, the trajectory, the transmit power of the UAV, and user scheduling. The contributions of this paper are listed as follows:

- We propose a secure RIS-assisted UAV-NOMA communication system adopting FBL transmission, where a UAV assisted by a RIS is used to transmit confidential messages to legitimate ground users in the presence of eavesdroppers.
- To maximize the average secrecy rate of ground users, we propose a joint optimization algorithm constrained to the mobility and transmit power of the UAV to optimize the phase shift of the RIS, the trajectory, the transmit power of the UAV, and the user scheduling.
- We formulate the optimization problem into four non-convex sub-problems, which are then transformed into four convex sub-problems by employing Taylor's first-order approximate expansion.
- We design an iterative algorithm by using successive convex approximation (SCA) to solve the approximate optimal solutions of the four sub-problems.

The remainder of this paper is organized as follows. In Sec. 2, the system model of secure RIS-assisted UAV-NOMA communication systems with FBL transmission is described. Then, the optimization problem is formulated. In Sec. 3, we decompose the formulated problem into four sub-problems and solve them via the developed alternating iterative algorithm. The numerical results are presented in Sec. 4, and Section 5 concludes this paper.

2. System Model

As illustrated in Fig. 1, we consider a RIS-assisted UAV-NOMA communication system, where a UAV, denoted as Alice, transmits messages to K ground users, denoted as Bobs, under the potential eavesdropper, denoted as Eve. In this scenario, Eve tries to intercept the communication between the UAV and the legitimate users. The UAV, the Eve, and K ground users are equipped with one antenna. Since the obstacles around ground users will affect the communication quality between the UAV and users, a RIS consisting of M reflecting elements, is deployed as a relay on the surface of a tall building to reflect UAV signals to users. In general, the controller on the RIS is directly connected to the UAV via a service channel. The UAV can transmit the location information obtained by its equipped sensors to the RIS controller timely over a service channel. Different from the conventional RIS-assisted UAV secure communication system, the proposed model considers the situation of CI possessing FBL. We use a three-dimensional (3D) cartesian coordinate system, where RIS, Eve, and users are situated on the ground plane at a height of 0, and their respective coordinates can be defined as $q_{\mathrm{r}} = [x_{\mathrm{r}}, y_{\mathrm{r}}]^{\mathrm{T}}$, $q_{\mathrm{e}} = [x_{\mathrm{e}}, y_{\mathrm{e}}]^{\mathrm{T}}$, and $q_k = [x_k, y_k]^{\mathrm{T}}$, $k\ (1 \le k \le K)$.

Define the trajectory of UAV as $q\ (t) = [x\ (t)\ , y\ (t)\ , H]$ with flight period T (s), where $0 \le t \le T$, and H (m) represents the minimum flight altitude of the UAV that required for realistic safety. T is divided into N equal time slots, e.g., $T = Nd_{\mathrm{t}}$, where d_{t} denotes the duration of each time slot.

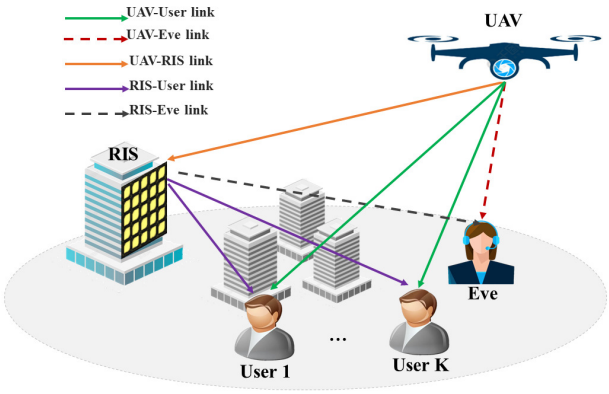

Fig. 1. Secure RIS-assisted UAV-NOMA communication system with FBL transmission, where the UAV transmits confidential messages to Users in the presence of the potential Eve, and RIS is deployed on the surface of the tall building to reflect the signals from the UAV to Users.

The length of d_t is chosen to be sufficiently small so that the location of the UAV can be considered unchanged within each time slot. Consequently, the trajectory of the UAV during the n-th time slot can be defined as $q[n] = [x(n), y(n), H]^T, 1 \le n \le N$, and the horizontal trajectory can be expressed as $q[n] = [x(n), y(n)]^T$.

The maximum flight speed of the UAV is defined as v_{max} [m/s]. Thus, the maximum distance that the UAV can fly in a time slot is $D = v_{max} d_t$. Suppose the UAV flies from an initial location $q_0 = [x_0, y_0, H]^T$ to an final location $q_f = [x_f, y_f, H]^T$. Then, the UAV mobility constraint after discretization can be expressed as

$$\|q[n+1] - q[n]\| \le v_{max} d_t, \quad n = 1, 2, \ldots, N-1, \quad (1)$$

and

$$q[1] = q_0, \quad q[N] = q_F. \quad (2)$$

2.1 Channel Model

In Fig. 1, the links from the UAV to ground nodes are assumed to be line-of-sight (LoS) channels following the free-space path loss model. Therefore, at n-th time slot, $h_k[n]$ is the channel gain between the UAV and the k-th user. $h_e[n]$ is the channel gain between the UAV and the Eve. Both $h_k[n]$ and $h_e[n]$ can be expressed by $h_\Psi[n], \Psi \in \{k, e\}$, which can be given by

$$h_\Psi[n] = \sqrt{\beta d_\Psi^{-2}[n]} = \sqrt{\frac{\beta}{H^2 + \|q[n] - q_\Psi\|^2}} \quad (3)$$

where β is the channel gain at the reference distance $d_0 = 1$ m, and the distance is $d_\Psi[n] = \sqrt{(x[n] - x_\Psi)^2 + (y[n] - y_\Psi)^2 + H^2}$ at n-th time slot.

Similarly, the channel gain from the UAV to RIS at n-th time slot can be described as

$$h_u[n] = \sqrt{\beta d_u^{-2}[n]} \left[1, e^{-j\frac{2\pi}{\lambda} l \cos\left(\varphi[n]^u_{AoA}\right)}, \ldots, e^{-j\frac{2\pi}{\lambda} l (M-1) \cos\left(\varphi[n]^u_{AoA}\right)}\right]^T \quad (4)$$

where λ and l are the carrier wavelength and the reflector spacing, respectively; $\cos\left(\varphi[n]^u_{AoA}\right)$ is the cosine of the angle of arrival (AoA) from UAV to RIS at n-th time slot.

Due to the presence of obstacles, the links from the RIS to users and Eve are assumed to be non-line-of-sight (NLOS) channels. Thus, the channel gain can be expressed as

$$h_\Phi[n] = \sqrt{\beta d_\Phi^{-\chi}[n]} \left[1, e^{-j\frac{2\pi}{\lambda} l \cos\left(\varphi[n]^\Phi_{AoD}\right)}, \ldots, e^{-j\frac{2\pi}{\lambda} l (M-1) \cos\left(\varphi[n]^\Phi_{AoD}\right)}\right]^T, \quad \Phi \in \{g, w\} \quad (5)$$

where $h_g[n]$ is the channel gain between the RIS and the k-th user and $h_w[n]$ is the channel gain between the RIS and Eve. χ denotes the path loss exponent; $d_\Phi[n]$ is the distance between the RIS and the k-th user or the Eve; $\cos\left(\varphi[n]^\Phi_{AoD}\right)$ is the cosine of the angle of departure (AoD) from RIS to k-th user or Eve at n-th time slot.

Therefore, in the n-th time slot, the signal $r_k[n]$ received at k-th user consists of the signal sent directly by the UAV and the signal reflected by the RIS, which can be given by

$$r_k[n] = \left(h_k[n] + h_g[n]^H \Theta[n] h_u[n]\right) \sqrt{p[n]} x_k[n] + N_k[n] \quad (6)$$

where $\Theta[n] = \text{diag}\left\{e^{j\theta_1[n]}, e^{j\theta_2[n]}, \ldots, e^{j\theta_M[n]}\right\}$ is the diagonal matrix of the RIS; $\theta_m[n] \in [0, 2\pi], m = \{1, 2, \ldots, M\}$ denotes the phase shift of the m-th reflecting elements at n-th time slot; $p_k[n]$ is the transmit power of the UAV and $x_k[n]$ is the signal sent by the UAV to k-th user at n-th time slot; $N_k[n]$ is the noise signal at the k-th user following the complex Gaussian distribution $\text{CN}(0, \sigma^2)$.

Considering the limitation of the average power and peak power [26], the transmit power constraints are given by

$$\frac{1}{N} \sum_{n=1}^{N} p[n] \le \bar{P}, \quad (7)$$

and

$$0 \le p[n] \le P_{peak} \quad (8)$$

where $\bar{P}$ and P_{peak} are the average and peak transmit power, respectively. Taking into account the validity of condition (7), we stipulate that $\bar{P} \le P_{peak}$. Since NOMA is adopted, all ground users can simultaneously be served with different frequency allocation levels. In this model, the UAV acts as a transmitter and employs SC to multiplex users. Additionally, SIC is utilized to detect the signals transmitted by different user receivers in ascending order of their respective channel gains. Therefore, the user signals with low channel gains are treated as interference to those with high channel gains. For simplicity, the variable $\alpha_{k,j}[n] \in \{0, 1\}$ is introduced. We define the k-th user as U_k, $\alpha_{k,j}[n] = 1$ indicates that U_j signal is considered as interference when decoding U_k signal since U_k has a better channel gain, otherwise $\alpha_{k,j}[n] = 0$. Accordingly, $\alpha_{k,j}[n]$ can be described as

$$\alpha_{k,j}[n] \in \{0, 1\}, \quad (9)$$

and

$$\alpha_{k,j}[n] \left(H^2 + \|q[n] - q_k\|^2\right) \le H^2 + \left\|q[n] - q_j\right\|^2. \quad (10)$$

Specifically,

$$\alpha_{k,k}[n] = 0, \quad (11)$$

and

$$\alpha_{k,j}[n] + \alpha_{j,k}[n] = 1, \forall k \ne j. \quad (12)$$

Equation (11) denotes that the UAV should not consider U_k signal as interference when decoding U_k signal. Equation (12) avoids the situation where two different users are considered as strong or weak users simultaneously.

According to [27] and [28], if the total ground interference is contained in Gaussian noise, the lower bound on the secrecy rate in bits per channel use (BPCU) at n-th time slot can be approximated as

$$R_{\text{sec}}[n] = \big[R_k[n] + R_{\text{g}}[n] - R_{\text{e}}[n] - R_{\text{w}}[n] - D_L(\varepsilon,\delta)\big]^+ \tag{13}$$

where $[x]^+ = \max\{x, 0\}$. $R_b[n]$ $(b \in \{k, e, g, w\})$ is expressed as

$$\begin{aligned} R_b[n] &= \log_2\left(1 + \frac{p[n]h_b[n]}{\sum\limits_{j=1}^{K}\alpha_{kj}p[n]h_j[n]+\sigma^2}\right) \\ &= \log_2\left(1 + \frac{p[n]\tilde{h}_b[n]}{1+\sum\limits_{j=1}^{K}\alpha_{kj}p[n]\tilde{h}_j[n]}\right) \end{aligned} \tag{14}$$

where $\tilde{h}_b[n] = \frac{h_b[n]}{\sigma^2}$, σ^2 represents the Gaussian noise variance in the transmission channel; and when $b = g, w$, $p[n] = p[n]\left(h_{\text{g}}[n]^{\text{H}}\Theta[n]\,h_{\text{u}}[n]\right)$.

In (13), $D_L(\varepsilon,\delta)$ can be given by

$$\begin{aligned} D_L(\varepsilon,\delta) = &\frac{Q^{-1}(\varepsilon)}{\ln 2}\left(\sqrt{\frac{V_k[n]}{L}} + \sqrt{\frac{V_{\text{g}}[n]}{L}}\right) \\ &+\frac{Q^{-1}(\delta)}{\ln 2}\left(\sqrt{\frac{V_{\text{e}}[n]}{L}} + \sqrt{\frac{V_{\text{w}}[n]}{L}}\right) \end{aligned} \tag{15}$$

where L is defined as the block length, $Q^{-1}(x)$ is the inverse of the Gaussian function $Q(x) \triangleq \int_x^\infty \frac{1}{\sqrt{2\pi}}\text{e}^{-\frac{t^2}{2}}\text{d}t$, ε and δ refer to the decoding error probability at users and the information leakage at Eves, respectively. $V_b[n]$ $(b \in \{k, e, g, w\})$ as the channel dispersion of the ground users and Eves at n-th time slot can be given by

$$V_b[n] = 1 - \left(1 + \frac{p[n]\,\tilde{h}_b[n]}{1+\sum\limits_{j=1}^{K}\alpha_{kj}p[n]\,\tilde{h}_j[n]}\right)^{-2}. \tag{16}$$

Note that in the case of FBL transmission, $D_L(\varepsilon,\delta)$ in (13) can be interpreted as penalties affecting the secrecy rate.

2.2 Problem Formulation

In this section, we formulate a joint optimization problem under the mobility constraint and the transmit power constraint of the UAV to maximize the average secrecy rate of all ground users by optimizing the phase shift of the RIS, the trajectory, the transmit power of the UAV, and the user scheduling.

Given the influence of FBL on the decoding error probability at users, the optimization problem is formulated as

$$(P1)\ \max_{Q,P,\Theta,A}\ \frac{1}{N}\sum_{n=1}^{N}\sum_{k=1}^{K}R_{\text{sec}}[n]\,(1-\varepsilon), \tag{17}$$

s.t.

$$\|q[n+1] - q[n]\| \le v_{\max}d_{\text{t}}, \tag{18}$$

$$q[1] = q_0, q[N] = q_{\text{F}}, \tag{19}$$

$$\frac{1}{N}\sum_{n=1}^{N}p[n] \le \bar{P}, \tag{20}$$

$$0 \le p[n] \le P_{\text{peak}}, \tag{21}$$

$$\theta_m[n] \in [0, 2\pi], m = \{1, 2, \ldots, M\}, \tag{22}$$

$$\alpha_{k,j}[n] \in \{0, 1\}, \tag{23}$$

$$\alpha_{k,k}[n] = 0, \tag{24}$$

$$\alpha_{k,j}[n] + \alpha_{j,k}[n] = 1, \forall k \ne j, \tag{25}$$

$$\alpha_{k,j}[n]\left(H^2 + \|q[n] - q_k\|^2\right) \le H^2 + \left\|q[n] - q_j\right\|^2, \forall k \ne j \tag{26}$$

where $A = \{\alpha_{k,j}[n], \forall k, j, n\}$, $P = \{p[n], \forall n\}$, $Q = \{q[n], \forall n\}$, and $\Theta = \{\theta_m[n], \forall m, n\}$. In (17), $p[n]$ can be set to 0 if $R_{\text{sec}}[n] < 0$ at n-th time slot, and then, $R_{\text{sec}}[n]$ increase towards 0 with satisfying (7) and (8). Consequently, the operation denoted by $[x]^+$ can be removed. Note that $(P1)$ is difficult to solve directly. In order to facilitate processing $(P1)$, we introduce the slack variables $U_b = \{u_b[n], \forall n\}$ and $Z_b = \{z_b[n], \forall n\}$, $b \in \{k, e, g, w\}$. Then, $(P1)$ can be reformulated as

$$(P2)\ \max_{Q,P,A,\Theta,U_b,Z_b}\ \frac{1}{N}\sum_{n=1}^{N}\sum_{k=1}^{K}\tilde{R}_{\text{sec}}[n]\,(1-\varepsilon), \tag{27}$$

s.t. (18)–(26)

$$u_b[n] \ge \frac{p[n]\,\tilde{h}_b[n]}{1+\sum\limits_{j=1}^{M}\alpha_{kj}p[n]\,\tilde{h}_j[n]}, \tag{28}$$

$$z_b^2[n] \ge 1 - (1 + u_b[n])^{-2}, \tag{29}$$

$$z_b[n] \ge 0 \tag{30}$$

where $\tilde{R}_{\text{sec}}[n]$ in (27) is given by

$$\begin{aligned} \tilde{R}_{\text{sec}}[n] = &\log_2(1 + u_k[n]) - \log_2(1 + u_{\text{e}}[n]) \\ &+ \log_2\left(1 + u_{\text{g}}[n]\right) - \log_2(1 + u_{\text{w}}[n]) \\ &- \left(z_k[n] + z_{\text{g}}[n]\right)\frac{Q^{-1}(\varepsilon)}{\sqrt{L}\ln 2} \\ &- \left(z_{\text{e}}[n] + z_{\text{w}}[n]\right)\frac{Q^{-1}(\delta)}{\sqrt{L}\ln 2} \end{aligned} \tag{31}$$

where $(P1)$ becomes simple to cope with due to (28). Equations (29) and (30) ensure the stable performance of the iterative algorithm proposed below. Furthermore, since (28) and (29) hold with equality at the optimal solution, $(P2)$ is equivalent to $(P1)$. However, $(P2)$ is non-convex and difficult to solve, and (28) and (29) are also non-convex. Therefore, we propose an iterative algorithm to decompose $(P2)$ into three subproblems, which are then transformed into convex problems to obtain the solution of $(P2)$.

3. Iteration Algorithm

The proposed optimization problem $(P2)$ is non-convex and difficult to be solved. Moreover, $(P2)$ contains four main variables (the phase shift Θ of the RIS, user scheduling A, the trajectory Q, and the transmit power P of the UAV). Therefore, we decompose $(P2)$ into four subproblems in this section. First, optimize Θ. Second, fix Θ, A and P to optimize Q. Third, fix Θ, Q and A to optimize P. Finally, fix Θ, Q and P to optimize A. The last three optimization subproblems are solved alternately until convergence.

3.1 Phase Shift Optimization

$h_{\mathrm{g}}[n]^{\mathrm{H}}\Theta\left[n\right]h_{\mathrm{u}}\left[n\right]$in (6) can be expressed as

$$h_{\mathrm{g}}[n]^{\mathrm{H}}\Theta\left[n\right]h_{\mathrm{u}}\left[n\right]=\frac{\beta\sum\limits_{m=1}^{M}\mathrm{e}^{\mathrm{j}\left[\theta_m[n]+\frac{2\pi}{\lambda}l(m-1)\left[\cos\left(\varphi[n]_{\mathrm{AoD}}^{\mathrm{g}}\right)-\cos\left(\varphi[n]_{\mathrm{AoA}}^{\mathrm{u}}\right)\right]\right]}}{\sqrt{d_{\mathrm{u}}^{-2}[n]d_{\mathrm{g}}^{-\chi}[n]}}. \tag{32}$$

Then, the phase shift of RIS can be denoted by

$$\begin{aligned}\theta_1\left[n\right]&=\theta_2\left[n\right]+\frac{2\pi}{\lambda}l\left[\cos\left(\varphi\left[n\right]_{\mathrm{AoD}}^{\mathrm{g}}\right)-\cos\left(\varphi\left[n\right]_{\mathrm{AoA}}^{\mathrm{u}}\right)\right]\\&=\ldots\\&=\theta_M\left[n\right]+\frac{2\pi}{\lambda}l\left(M-1\right)\\&\quad\cdot\left[\cos\left(\varphi\left[n\right]_{\mathrm{AoD}}^{\mathrm{g}}\right)-\cos\left(\varphi\left[n\right]_{\mathrm{AoA}}^{\mathrm{u}}\right)\right]\\&=\omega\end{aligned} \tag{33}$$

where $\omega=[0,2\pi]$ is the direction to aim. Therefore, the phase shift of the m-th reflecting element of the RIS can be expressed as:

$$\begin{aligned}\theta_m\left[n\right]=&\frac{2\pi}{\lambda}l\left(m-1\right)\left[\cos\left(\varphi\left[n\right]_{\mathrm{AoA}}^{\mathrm{u}}\right)-\cos\left(\varphi\left[n\right]_{\mathrm{AoD}}^{\mathrm{g}}\right)\right]\\&+\omega.\end{aligned} \tag{34}$$

Then, the maximum value can be approximated by the upper bound of $\left|h_{\mathrm{g}}[n]^{\mathrm{H}}\Theta\left[n\right]h_{\mathrm{u}}\left[n\right]\right|^2$, which can be obtained by substituting (34) into (32) and can be given by

$$\begin{aligned}&\left|h_{\mathrm{g}}[n]^{\mathrm{H}}\Theta\left[n\right]h_{\mathrm{u}}\left[n\right]\right|^2\\&=\left|\frac{\beta\sum\limits_{m=1}^{M}\mathrm{e}^{\mathrm{j}\left[\theta_m[n]+\frac{2\pi}{\lambda}l(m-1)\left[\cos\left(\varphi[n]_{\mathrm{AoD}}^{\mathrm{g}}\right)-\cos\left(\varphi[n]_{\mathrm{AoA}}^{\mathrm{u}}\right)\right]\right]}}{\sqrt{d_{\mathrm{u}}^{-2}[n]d_{\mathrm{g}}^{-\chi}[n]}}\right|^2\\&=\left|\frac{\beta M\mathrm{e}^{\mathrm{j}\omega}}{\sqrt{d_{\mathrm{u}}^{-2}[n]d_{\mathrm{g}}^{-\chi}[n]}}\right|^2\leq\frac{\beta^2M^2}{d_{\mathrm{u}}^{-2}[n]d_{\mathrm{g}}^{-\chi}[n]}.\end{aligned} \tag{35}$$

Thus, the best Θ can be obtained by phase alignment.

3.2 Trajectory Optimization

Given Θ, A and P, $(P2)$ can be simplified as

$$\begin{aligned}(P3)\ &\max_{Q,U_b,Z_b}\frac{1}{N}\sum_{n=1}^{N}\sum_{k=1}^{K}\tilde{R}_{\mathrm{sec}}\left[n\right](1-\varepsilon),\\&\text{s.t. (18), (19), (28)–(30).}\end{aligned} \tag{36}$$

Since (28) and (29) are non-convex, (36) is non-convex. Next, we transform $(P3)$ into a convex optimization problem. According to the trajectory optimization, equation (28) can be expressed as

$$u_b\left[n\right]\geq\frac{\frac{r_0P_k}{H^2+\|q[n]-q_k\|^2}}{1+\sum\limits_{j=1}^{K}\frac{r_0\alpha_{k,j}P_k}{H^2+\|q[n]-q_k\|^2}} \tag{37}$$

where $r_0=\frac{\beta}{\sigma^2}$. With the slack variables $L_b=\{l_b\left[n\right],\forall n\}$ and $M_b=\{m_b\left[n\right],\forall n\},b\in\{k,e,g,w\}$, equation (37) can be rewritten as

$$u_b\left[n\right]\geq\frac{l_b\left[n\right]}{m_b\left[n\right]} \tag{38}$$

where

$$\frac{r_0P_k}{H^2+\|q[n]-q_k\|^2}\geq l_b\left[n\right] \tag{39}$$

and

$$1+\sum_{j=1}^{K}\frac{r_0\alpha_{k,j}P_k}{H^2+\|q[n]-q_k\|^2}\leq m_b\left[n\right]. \tag{40}$$

Then, equation (38) is convex. However, equations (39) and (40) are still non-convex. Since the convex function can be obtained by expanding the first-order Taylor's formula, equation (39) can be converted to

$$\begin{aligned}l_b\left[n\right]\leq&\frac{r_0P_k}{H^2+\|\hat{q}[n]-q_k\|^2}-\\&\frac{2(\hat{q}[n]-q_k)^{\mathrm{T}}\left(q\left[n\right]-\hat{q}\left[n\right]\right)r_0P_k}{\left(H^2+\|\hat{q}[n]-q_k\|^2\right)^2}.\end{aligned} \tag{41}$$

With the variable $Y_b\left[n\right]=\{y_b\left[n\right],\forall n\}$, equation (40) can be transformed to

$$1+\sum_{j=1}^{K}y_b[n]\leq m_b\left[n\right] \tag{42}$$

where

$$\frac{r_0\alpha_{k,j}P_k}{H^2+\|q[n]-q_k\|^2}\geq y_b[n]. \tag{43}$$

By employing the first-order Taylor expansion, equation (43) is given by

$$y_b[n] \leq \frac{r_0\alpha_{k,j}P_k}{H^2+\|\hat{q}[n]-q_k\|^2} - \frac{2(\hat{q}[n]-q_k)^{\mathrm{T}}(q[n]-\hat{q}[n])r_0\alpha_{k,j}P_k}{\left(H^2+\|\hat{q}[n]-q_k\|^2\right)^2}. \quad (44)$$

Equation (37) is successfully converted to a convex constraint according to the transformation of (39) and (40). Consequently, given points $\hat{z}_b[n]$ and $\hat{u}_b[n]$, equation (29) can be approximated as

$$\hat{z}_b^2[n] + 2\hat{z}_b[n](z_b[n]-\hat{z}_b[n]) \geq 1 - (1+\hat{u}_b[n])^{-2} + 2(1+\hat{u}_b[n])^{-3}(u_b[n]-\hat{u}_b[n]). \quad (45)$$

Due to the usage of slack variables $m_b[n]$ and $l_b[n]$, combining (39) and (40), $\tilde{R}_{\mathrm{sec}}[n]$ can be rewritten as

$$\tilde{R}_{\mathrm{sec}}[n] = \sum_{b=k,g}\log_2\left(1+\frac{l_b[n]}{m_b[n]}\right) - \sum_{b=e,w}\log_2\left(1+\frac{l_b[n]}{m_b[n]}\right) - \frac{\left[(z_k[n]+z_g[n])Q^{-1}(\varepsilon)+(z_e[n]+z_w[n])Q^{-1}(\delta)\right]}{\sqrt{L}\ln 2}. \quad (46)$$

Therefore, given the points $\hat{l}_b[n]$ and $\hat{m}_b[n]$, the first-order Taylor expansion of (46) can be used to construct the lower bound of $\tilde{R}_{\mathrm{sec}}[n]$, denoted as $R^{\mathrm{lb}}_{\mathrm{sec},q}[n]$.

After the above transformations, $(P3)$ can be reformulated as

$$(P4)\ \max_{Q,U_b,Z_b,L_b,M_b,Y_b}\frac{1}{N}\sum_{n=1}^{N}\sum_{k=1}^{K}R^{\mathrm{lb}}_{\mathrm{sec},q}[n](1-\varepsilon), \quad (47)$$
$$\text{s.t. (18), (19), (38), (41), (42), (44), (45).}$$

Hence, $(P4)$ is a convex optimization problem that can be solved efficiently by optimization tools, such as CVX.

3.3 Transmit Power Optimization

Given Θ, A and Q, the optimization problem $(P2)$ can be simplified as

$$(P5)\ \max_{Q,U_b,Z_b}\frac{1}{N}\sum_{n=1}^{N}\sum_{k=1}^{K}\tilde{R}_{\mathrm{sec}}[n](1-\varepsilon), \quad (48)$$
$$\text{s.t. (20), (21), (28)–(30).}$$

$(P5)$ is non-convex due to the non-convexity of (29). Similar to the process in Sec 3.2., equation (29) can be converted to (45), and the lower bound of $\tilde{R}_{\mathrm{sec}}[n]$ in (48) that constructed by employing the first-order approximation is given by

$$\tilde{R}_{\mathrm{sec}}[n] \geq \sum_{b=k,g}\log_2\left(1+\frac{p[n]\tilde{h}_b[n]}{1+\sum_{j=1}^{K}\alpha_{kj}p[n]\tilde{h}_j[n]}\right) - \sum_{b=e,w}\left[\log_2(1+\hat{u}_b[n]) - \frac{u_b[n]-\hat{u}_b[n]}{(1+\hat{u}_b[n])\ln 2}\right] - \frac{(z_k[n]+z_g[n])Q^{-1}(\varepsilon)+(z_e[n]+z_w[n])Q^{-1}(\delta)}{\sqrt{L}\ln 2} \triangleq \tilde{R}^{\mathrm{lb}}_{\mathrm{sec},p}[n]. \quad (49)$$

Thus, $(P5)$ can be approximated as

$$(P6)\ \max_{P,U_b,Z_b}\frac{1}{N}\sum_{n=1}^{N}\sum_{k=1}^{K}R^{\mathrm{lb}}_{\mathrm{sec},p}[n](1-\varepsilon), \quad (50)$$
$$\text{s.t. (20), (21), (28), (30), (45).}$$

After transformation, $(P6)$ is convex and can be solved efficiently with CVX.

3.4 User Scheduling Optimization

Given Θ, P and Q, the optimization problem $(P2)$ can be simplified as

$$(P7)\ \max_{\mathrm{A},U_b,Z_b}\frac{1}{N}\sum_{n=1}^{N}\sum_{k=1}^{K}\tilde{R}_{\mathrm{sec}}[n](1-\varepsilon), \quad (51)$$
$$\text{s.t. (23)–(26), (28)–(30).}$$

Owing to the non-convexity of (26) and (29), $(P7)$ is a non-convex optimization problem. First, equation (23) is effectively equivalent to

$$0 \leq \alpha_{k,j}[n] \leq 1, \quad (52)$$

and

$$\sum_{n=1}^{N}\sum_{k,j}^{K}\left(\alpha_{k,j}[n]-{\alpha^2}_{k,j}[n]\right) \leq 0. \quad (53)$$

Due to the non-convexity of ${\alpha^2}_{k,j}[n]$, equation (53) remains non-convex. The utilization of the first-order approximation is impractical in $(P7)$ due to (52) and (53) [29]. By employing slack variable ϕ, $(P7)$ can be rewritten as

$$(P8)\ \max_{\mathrm{A},U_b,Z_b,\phi}\frac{1}{N}\sum_{n=1}^{N}\sum_{k=1}^{K}\tilde{R}_{\mathrm{sec}}[n](1-\varepsilon) - \lambda\phi, \quad (54)$$
$$\text{s.t. (24)–(26), (28)–(30), (52)}$$

when $\lambda \geq \lambda^*$, $\phi \triangleq \sum_{n=1}^{N}\sum_{k,j}^{K}\left(\alpha_{k,j}[n]-\alpha^2_{k,j}[n]\right)$, λ^* is the optimal Lagrange multiplier associated with (53). When $\phi = 0$ at the point of convergence, $(P8)$ is equivalent to $(P7)$ [30]. For any localized point $\{\bar{\alpha}_{k,j}[n]\}$, the upper bound of ϕ can be obtained as

$$\phi \leq \sum_{n=1}^{N}\sum_{k,j}^{K}\left(\alpha_{k,j}[n]+\bar{\alpha}^2_{k,j}[n]-2\bar{\alpha}_{k,j}[n]\,{\alpha^2}_{k,j}[n]\right) \triangleq \bar{\phi}. \quad (55)$$

Till now, equation (26) can be rewritten as

$$\frac{\left(H^2+\|q[n]-q_k\|^2+\alpha_{k,j}\right)^2}{4} \leq H^2+\left\|q[n]-q_j\right\|^2+\frac{\left(H^2+\|q[n]-q_k\|^2-\alpha_{k,j}\right)^2}{4}, \forall k \neq j. \quad (56)$$

Both the left and right of (56) are convex with respect to $\alpha_{k,j}[n]$. Similar to (55), by employing the first-order approximation, equation (56) can be reformulated as

$$\begin{aligned}&\frac{\left(H^2+\|q[n]-q_k\|^2+\alpha_{k,j}\right)^2}{4}+\frac{\left(H^2+\|q[n]-q_k\|^2-\bar{\alpha}_{k,j}\right)^2}{4}\\&\leq\frac{\left(H^2+\|q[n]-q_k\|^2-\bar{\alpha}_{k,j}\right)\left(H^2+\|q[n]-q_k\|^2-\alpha_{k,j}\right)}{2}\\&\quad+H^2+\left\|q\left[n\right]-q_j\right\|^2,\forall k\neq j.\end{aligned}\tag{57}$$

By employing the first-order Taylor expansion, we can construct the lower bound of $\tilde{R}_{\text{sec}}[n]$, denoted as $\tilde{R}^{\text{lb}}_{\text{sec},A}[n]$.

Thus, $(P7)$ can be approximated as

$$(P9)\ \max_{\text{A},U_b,Z_b,\phi}\ \frac{1}{N}\sum_{n=1}^{N}\sum_{k=1}^{K}\tilde{R}^{\text{lb}}_{\text{sec},A}[n]\,(1-\varepsilon)-\lambda\bar{\phi},\tag{58}$$

s.t. (24), (25), (28), (30), (45),(52), (57).

Therefore, $(P9)$ is a convex optimization problem that can be solved efficiently with CVX.

3.5 Algorithm Design

In this section, an iterative algorithm based on SCA is designed to optimize the subproblems alternately with the optimal phase shift of the RIS. According to the principle of SCA, in each iteration, the current optimal solution of each subproblem gradually approaches the solution of $(P1)$. Details of the algorithm are presented in Algorithm 1. Furthermore, the objective value of $(P1)$ is bounded and non-decreasing at each iteration, ensuring the convergence of Algorithm 1. However, the iterative algorithm only guarantees the global solution to the convex optimization problem. With the processing of the above three subsections, the optimal objective values of $(P4)$, $(P6)$, and $(P9)$ serve as lower bounds for $(P3)$, $(P5)$, and $(P7)$, respectively. Due to the first-order Taylor approximation, which leads to a stringent feasible set, Algorithm 1 can only obtain a suboptimal solution to $(P1)$.

Algorithm 1. Iterative optimization algorithm.

Initialize $\{Q^0,\Theta^0,P^0,\text{A}^0,U_k^0,Z_k^0\}$, $m=0$, η, number of iterations $r=0$
The optimal Θ is obtained according to (33)
repeat
  Update $\{Q^{r+1},U_b^{r+1},Z_b^{r+1}\}$ based on $(P4)$ with given $\{\Theta,P^r,A^r,U_b^r,Z_b^r\}$.
  $\{U_b^r,Z_b^r\}=\{U_b^{r+1},Z_b^{r+1}\}$.
  Update $\{P^{r+1},U_b^{r+1},Z_b^{r+1}\}$ based on $(P6)$ with given $\{\Theta,Q^{r+1},A^r,U_b^r,Z_b^r\}$.
  $\{U_b^r,Z_b^r\}=\{U_b^{r+1},Z_b^{r+1}\}$.
  Update $\{A^{r+1},U_b^{r+1},Z_b^{r+1}\}$ based on $(P9)$ with given $\{\Theta,Q^{r+1},P^{r+1},U_b^r,Z_b^r\}$.
  Update $r=r+1$, $m=m+1$, $\lambda^{m+1}=\min\{c\lambda^m,\lambda_{\max}\}$.
until $\phi\leq\eta$, the fraction of the objective value grows below the threshold value τ.

Moreover, a penalty parameter λ is adopted in user scheduling optimization to cope with (23). To expand the feasible set, in Algorithm 1, we set λ_0 as a sufficiently small initial value, and then update λ stepwise with a constant c until λ reaches the corresponding bound $\lambda_{\max}$, guaranteeing that $\phi\to 0$ upon convergence.

4. Numerical Results

In this paper, we have proposed a RIS-assisted UAV-NOMA communication system with FBL transmission. To evaluate the performance of the proposed optimization scheme (denoted as RIS-assisted UAV-NOMA with FBL), the numerical results are presented in this section. Assume that there are 3 ground users distributed in one plane simultaneously. The parameters are listed in Tab. 1. For comparison, six additional benchmark schemes are considered: RIS-assisted UAV-NOMA with IBL, which serves as a RIS-assisted UAV-NOMA communication scheme for transmitting IBL packets; RIS-assisted UAV-TDMA with FBL, a RIS-assisted UAV communication scheme for the transmission of FBL packets, employing time division multiple access (TDMA) methodology; UAV-NOMA with FBL, a UAV-NOMA communication scheme for transmitting FBL packets; UAV-TDMA with FBL, a UAV-TDMA communication scheme with FBL transmission. The straight UAV-NOMA with FBL scheme is a NOMA communication scheme

Parameter	Meaning	Value
q_0, q_{f}	Initial position and final position coordinates of the UAV	$[0,-200,50]^{\text{T}}$ m, $[0,200,50]^{\text{T}}$ m
q_{e}	Position coordinates of the Eve	$[90,50]^{\text{T}}$ m
H	Altitude of the UAV	100 m
$V_{\max}$	Maximum speed of the UAV	20 m/s
d_{t}	Time slot length	1 s
P_{peak}	Maximum power	20 dBm
σ^2	Noise power	–60 dBm
L	Finite block length	400
ε	Decoding error probability	10^{-5}
δ	Information leakage	10^{-2}
M	Number of IRS reflecting elements	30
χ	Path loss exponent	2.2

Tab. 1. Parameter settings in numerical analysis.

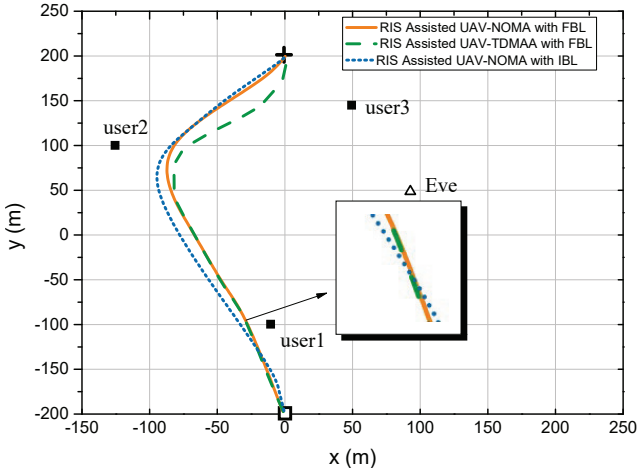

Fig. 2. Horizontal trajectory of UAV for different schemes at period $T = 45$ s.

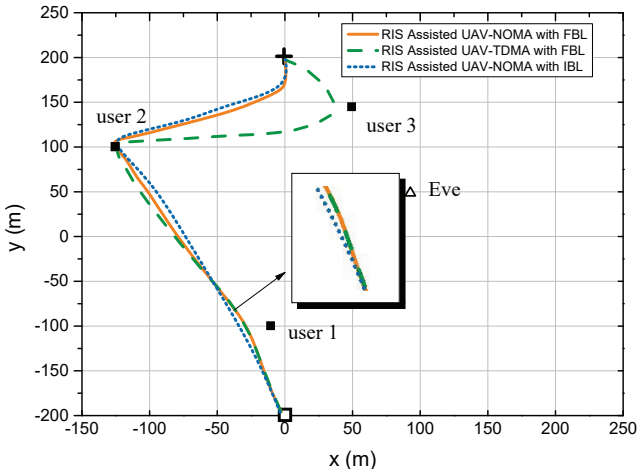

Fig. 3. Horizontal trajectories of UAVs in different schemes at period $T = 100$ s.

for FBL transmission without the UAV's transmit power optimization, and the straight UAV-TDMA with FBL is a TDMA communication scheme for FBL transmission without optimizing the transmission power of the UAV.

Figures 2 and 3 show the horizontal trajectory of the UAV at different periods under RIS-assisted UAV-NOMA with FBL, RIS-assisted UAV-NOMA with IBL, and RIS-assisted UAV-TDMA with FBL schemes. First, in Fig. 2, $T = 45$ s is insufficient for the UAV moving to the users. UAVs only approach users in the three schemes with slightly different trajectories. In contrast, a more suitable flight period is adopted in Fig. 3, which enables the UAV to reach the location of users. Second, When the UAV travels close to a user, the NOMA scheme is more alert to Eve than the TDMA scheme. The differences arise from the fact that according to the time resource allocation strategy in TDMA, the UAV communicates exclusively with the nearest user in a time slot. Therefore, the UAV can meet the requirement of the minimum average secrecy rate by moving close to the user to obtain better channel quality. Consequently, the trajectory of the UAV in TDMA is bound to be closer to Eve than

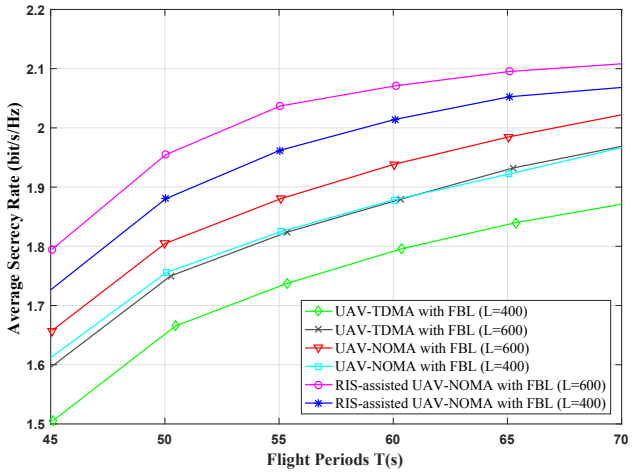

Fig. 4. Average secrecy rate versus flight periods T under different block lengths L.

NOMA, potentially exposing more signals to Eve. However, after UAV moves away from Eve, the trajectories of all schemes are similar. Third, We can observe that the trajectories of all three schemes are similar regardless of the adequacy of the flight period. Thus, the proposed RIS-assisted UAV-NOMA with FBL scheme in this paper effectively harmonizes user security and fairness, guaranteeing the average secrecy rate of each user.

Figure 4 demonstrates the average secrecy rate of RIS-assisted UAV-NOMA with FBL, UAV-NOMA with FBL, and UAV-TDMA with FBL versus different flight periods T and different block lengths L. First, the average secrecy rate of the three schemes escalates as T increases. The reason is that a higher average secrecy rate can be obtained since the UAV stays longer in the hovering location with a larger T. Second, in the same scheme with a given flight period T, the higher average secrecy rate can be obtained with the larger L. This is due to the fact that L as the finite block constraint is located at the denominator of the subtracted number in the optimization formula, and L has the same monotonic change trend as the average secrecy rate. Third, the NOMA scheme outperforms the TDMA scheme due to the change of transmission mode. Furthermore, with the same L, the proposed RIS-assisted UAV-NOMA with FBL scheme can improve the average secrecy rate by about 12 to 20 percent compared to UAV-NOMA with FBL.

Figure 5 illustrates the average secrecy rate versus the threshold τ for different optimization schemes with $T = 45$ s and the transmit power of the UAV $P_{\max} = 0.1$ W. When τ is relatively low, the average secrecy rate achieved by all schemes increases rapidly. However, as τ increases, the rate of average secrecy rate increment begins to decelerate smoothly. The reason is that when τ is small, the transmit power of the UAV gradually increases, leading to a rise in the secrecy rate. Nevertheless, as τ creases, the transmit power is limited by P_{peak} to satisfy the maximum power constraint. Moreover, in conjunction with Fig. 4, the NOMA scheme consistently achieves a higher average secrecy rate than the

TDMA scheme under the FBL transmission, which validates the importance of jointly optimizing the trajectory and transmit power of the UAV. Furthermore, we can observe that the security performance of the proposed UAV-NOMA communication system has been significantly improved with the assistance of the RIS.

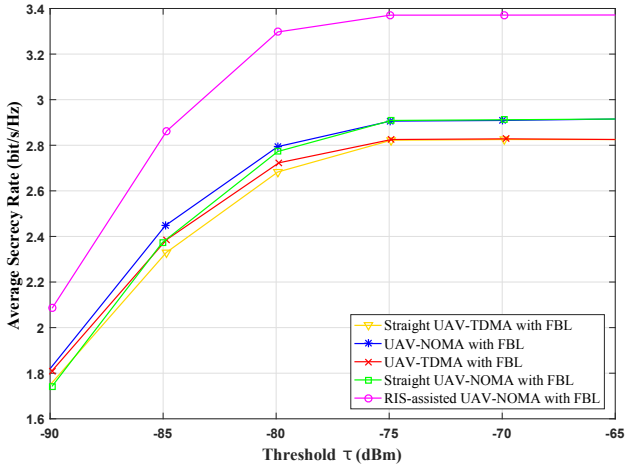

Fig. 5. Average secrecy rate versus threshold value for $T = 45$ s and $P_{\max} = 0.1$ W.

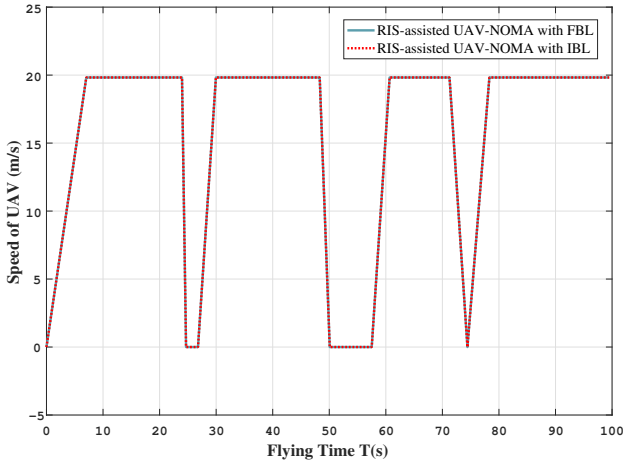

Fig. 6. Flight speed of the UAV when $T = 100$ s.

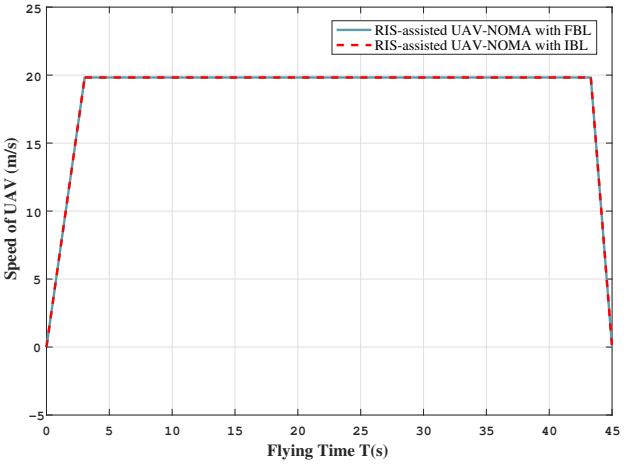

Fig. 7. Flight speed of the UAV when $T = 45$ s.

Figures 6 and 7 depict the flight speed of the UAV combined with the trajectory under the RIS-assisted UAV-NOMA scheme. The speed of the UAV reduces to 0 to transmit more messages via a better air-to-ground channel when it flies close to users. First, when $T = 100$ s in Fig. 6, the speed of the UAV varies with time, hovering in sequential proximity to users to enjoy the best communication channel. Combined with Fig. 3, it can be seen that the hovering location is exactly near to users but far away from Eve. Since User 2 is farthest from Eve, the UAV hovers for the longest time at $t = 45$ s. Conversely, it hovers for the shortest time around User 3 being closest to Eve. Therefore, the hovering position is a trade-off between communication performance and security performance. Second, as shown in Fig. 7, when $T = 45$ s, the UAV always flies from the initial to final positions at the maximum speed with a curved flight path to be as close as possible to each user in each finite period. Furthermore, from Figs. 6 and 7, we observed that RIS-assisted UAV-NOMA with FBL and RIS-assisted UAV-NOMA with IBL exhibit near-identical results in terms of flight speed and trajectory for UAVs.

5. Conclusions

In this paper, we have proposed a secure RIS-assisted UAV-NOMA communication system adopting FBL transmission. To maximize the average secrecy rate, we formulate the optimization problem to jointly optimize the phase shift of the RIS, the trajectory, the transmit power of the UAV, and the user scheduling under the mobility and power constraints of the UAV. Since the optimization problem is non-convex and hard to be solved, we have first decomposed the formulated problem into four sub-problems, i.e., phase shift optimization, trajectory optimization, transmit power optimization, and user scheduling optimization. Then, these four non-convex sub-problems have been transformed into four convex sub-problems by utilizing Taylor's first-order expansion. Finally, an iterative algorithm based on SCA is designed to solve the four sub-problems to obtain the sub-optimal solution of the optimization problem. Numerical results show that the performance of the proposed joint optimization scheme is significantly better than the traditional schemes.

Abbreviations

The following abbreviations are used in this manuscript:

- Unmanned aerial vehicle (UAV)
- Quality of service (QoS)
- 5th generation (5G)
- Base station (BS)
- Reconfigurable intelligent surface (RIS)
- Physical layer security (PLS)
- Eavesdropper (Eve)

- Non-orthogonal multiple access (NOMA)
- Superposition coding (SC)
- Successive interference cancellation (SIC)
- Confidential information (CI)
- Infinite blocklength (IBL)
- Finite blocklength (FBL)
- Successive convex approximation (SCA)
- Three-dimensional (3D)
- Line-of-Sight (LoS)
- Bits per channel use (BPCU)
- Time division multiple access (TDMA)

References

[1] QIAN, Y., WANG, F., LI, J., et al. User association and path planning for UAV-aided mobile edge computing with energy restriction. *IEEE Wireless Communications Letters*, 2019, vol. 8, no. 5, p. 1312–1315. DOI: 10.1109/LWC.2019.2913843

[2] CHEN, X., CHANG, Z., LIU, M., et al. UAV-IRS assisted covert communication: Introducing uncertainty via phase shifting. *IEEE Wireless Communications Letters*, 2024, vol. 13, no. 1, p. 103–107. DOI: 10.1109/LWC.2023.3321957

[3] BERA, A., MISRA, S., CHATTERJEE, C. QoE analysis in cache-enabled multi-UAV networks. *IEEE Transactions on Vehicular Technology*, 2020, vol. 69, no. 6, p. 6680–6687. DOI: 10.1109/TVT.2020.2985933

[4] DING, Y., FENG, Y., LU, W., et al. Online edge learning offloading and resource management for UAV-assisted MEC secure communications. *IEEE Journal of Selected Topics in Signal Processing*, 2023, vol. 17, no. 1, p. 54–65. DOI: 10.1109/JSTSP.2022.3222910

[5] CHEN, X., ZHANG, N., TANG, J., et al. UAV-aided covert communication with a multi-antenna jammer. *IEEE Transactions on Vehicular Technology*, 2021, vol. 70, no. 11, p. 11619–11631. DOI: 10.1109/TVT.2021.3112121

[6] HUANG, J., TIAN, G., ZHANG, J., et al. On unmanned aerial vehicles light show systems: Algorithms, software and hardware. *Applied Sciences*, 2021, vol. 11, no. 16, p. 1–19. DOI: 10.3390/app11167687

[7] YE, J., FU, C., CAO, Z., et al. Tracker meets night: A transformer enhancer for UAV tracking. *IEEE Robotics and Automation Letters*, 2022, vol. 7, no. 2, p. 3866–3873. DOI: 10.1109/LRA.2022.3146911

[8] JIANG, X., YANG, Z., ZHAO, N., et al. Resource allocation and trajectory optimization for UAV-enabled multi-user covert communications. *IEEE Transactions on Vehicular Technology*, 2021, vol. 70, no. 2, p. 1989–1994. DOI: 10.1109/TVT.2021.3053936

[9] WANG, J., WANG, X., GAO, R., et al. Physical layer security for UAV communications: A comprehensive survey. *China Communications*, 2022, vol. 19, no. 9, p. 77–115. DOI: 10.23919/JCC.2022.09.007

[10] ZHOU, X., YAN, S., WU, Q., et al. Intelligent reflecting surface (IRS)-aided covert wireless communications with delay constraint. *IEEE Transactions on Wireless Communications*, 2022, vol. 21, no. 1, p. 532–547. DOI: 10.1109/TWC.2021.3098099

[11] LIN, Y., SHU, F., DONG, R., et al. Enhanced-rate iterative beamformers for active IRS-assisted wireless communications. *IEEE Wireless Communications Letters*, 2023, vol. 12, no. 9, p. 1538–1542. DOI: 10.1109/LWC.2023.3281821

[12] LIU, X., YU, Y., LI, F., et al. Throughput maximization for RIS-UAV relaying communications. *IEEE Transactions on Intelligent Transportation Systems*, 2022, vol. 23, no. 10, p. 19569–19574. DOI: 10.1109/TITS.2022.3161698

[13] QIAN, Y., YANG, C., MEI, Z., et al. On joint optimization of trajectory and phase shift for IRS-UAV assisted covert communication systems. *IEEE Transactions on Vehicular Technology*, 2023, vol. 72, no. 10, p. 12873–12883. DOI: 10.1109/TVT.2023.3271461

[14] SHU, F., TENG, Y., LI, J., et al. Enhanced secrecy rate maximization for directional modulation networks via IRS. *IEEE Transactions on Communications*, 2021, vol. 69, no. 12, p. 8388–8401. DOI: 10.1109/TCOMM.2021.3110598

[15] CUI, M., ZHANG, G., ZHANG, R. Secure wireless communication via intelligent reflecting surface. *IEEE Wireless Communications Letters*, 2019, vol. 8, no. 5, p. 1410–1414. DOI: 10.1109/LWC.2019.2919685

[16] FANG, S., CHEN, G., LI, Y. Joint optimization for secure intelligent reflecting surface assisted UAV networks. *IEEE Wireless Communications Letters*, 2021, vol. 10, no. 2, p. 276–280. DOI: 10.1109/LWC.2020.3027969

[17] PANG, X., ZHAO, N., TANG, J., et al. IRS-assisted secure UAV transmission via joint trajectory and beamforming design. *IEEE Transactions on Communications*, 2022, vol. 70, no. 2, p. 1140–1152. DOI: 10.1109/TCOMM.2021.3136563

[18] ZHAI, D., LI, H., TANG, X., et al. Height optimization and resource allocation for NOMA enhanced UAV-aided relay networks. *IEEE Transactions on Communications*, 2021, vol. 69, no. 2, p. 962–975. DOI: 10.1109/TCOMM.2020.3037345

[19] LIU, M., YANG, J., GUI, G. DSF-NOMA: UAV- assisted emergency communication technology in a heterogeneous internet of things. *IEEE Internet of Things Journal*, 2019, vol. 6, no. 3, p. 5508–5519. DOI: 10.1109/JIOT.2019.2903165

[20] CAI, Y., WEI, Z., HU, S., et al. Resource allocation and 3D trajectory design for power-efficient IRS-assisted UAV-NOMA communications. *IEEE Transactions on Wireless Communications*, 2022, vol. 21, no. 12, p. 10315–10334. DOI: 10.1109/TWC.2022.3183300

[21] MU, X., LIU, Y., GUO, L., et al. Intelligent reflecting surface enhanced multi-UAV NOMA networks. *IEEE Journal on Selected Areas in Communications*, 2021, vol. 39, no. 10, p. 3051–3066. DOI: 10.1109/JSAC.2021.3088679

[22] BEAK, J., HAN, S. I., HAN, Y. Optimal resource allocation for non-orthogonal transmission in UAV relay systems. *IEEE Wireless Communications Letters*, 2018, vol. 7, no. 3, p. 356–359. DOI: 10.1109/LWC.2017.2778073

[23] WANG, Y., ZHOU, X. ZHUANG, Z., et al. UAV-enabled secure communication with finite blocklength. *IEEE Transactions on Vehicular Technology*, 2020, vol. 69, no. 12, p. 16309–16313. DOI: 10.1109/TVT.2020.3042791

[24] SINGH, S. K., AGRAWAL, K., SINGH, K., et al. Performance analysis and optimization of RSMA enabled UAV-aided IBL and FBL communication with imperfect SIC and SCI. *IEEE Transactions on Wireless Communications*, 2023, vol. 22, no. 6, p. 3714–3732. DOI: 10.1109/TWC.2022.3220785

[25] AGRAWAL, N., BANSAL, A., SINGH, K., et al. Finite block length analysis of RIS-assisted UAV-based multiuser IOT communication system with non-linear EH. *IEEE Transactions on Communications*, 2020, vol. 70, no. 5, p. 3542–3557. DOI: 10.1109/TCOMM.2022.3162249

[26] HAN, H., HUANG, Y., HU, H., et al. Mobile jammer enabled secure UAV communication with short packet transmission. *AEU - International Journal of Electronics and Communications*, 2022, vol. 157, p. 1–10. DOI: 10.1016/j.aeue.2022.154434

[27] YANG, W., SCHAEFER, R. F., POOR, H. V. Finite-blocklength bounds for wiretap channels. In *IEEE International Symposium on Information Theory (ISIT)*. Barcelona (Spain), 2016, p. 3087–3091. DOI: 10.1109/ISIT.2016.7541867

[28] WANG, H., YANG, Q., DING, Z., et al. Secure short-packet communications for mission-critical IOT applications. *IEEE Transactions on Wireless Communications*, 2019, vol. 18, no. 5, p. 2565–2578. DOI: 10.1109/TWC.2019.2904968

[29] ZHANG, J., CHEN, X., LI, M., et al. Optimized throughput in covert millimeter-wave UAV communications with beam sweeping. *IEEE Wireless Communications Letters*, 2021, vol. 10, no. 4, p. 720–724. DOI: 10.1109/LWC.2020.3041637

[30] TANG, R., CHENG, J., CAO, Z. Joint placement design, admission control, and power allocation for NOMA-based UAV systems. *IEEE Wireless Communications Letters*, 2020, vol. 9, no. 3, p. 385–388. DOI: 10.1109/LWC.2019.2956702

About the Authors ...

Dan ZHAO received the master's degree from the School of Communication and Information Engineering, at Nanjing University of Posts and Telecommunications, Nanjing, China, in 2008. From 2008 to 2014, she worked as an engineer in H3C. Since 2016, she has been a Lecturer with the School of Electric and Optical Engineering, at Nanjing University of Science and Technology ZiJin College.

Linzi HU received the B.S. degree from the School of Electronic and Optical Engineering, at Nanjing University of Science and Technology in 2022, where she is currently working toward the M.S. degree. Her research interests include reinforcement learning, deep learning, and UAV communication.

Wei XIONG received the master's degree from the School of Electronic and Optical Engineering, at Nanjing University of Science and Technology in 2023.

Huan CAI received the B.S. degree from the School of Electronic and Optical Engineering, at Nanjing University of Information Science and Technology in 2022. Since 2022, he has worked toward the M.S. degree at Nanjing University of Science and Technology. His research interests include covert communications, deep learning, and UAV communication.

Yuwen QIAN (corresponding author) received his Ph.D. degree in Automatic Engineering from the Nanjing University of Science and Technology, Nanjing, China, in 2011. From 2002 to 2011, he was a Lecturer at the School of Automation, Nanjing University of Science and Technology. Since 2019, he has been an Associate Professor with the School of Electronic and Optical Engineering, at Nanjing University of Science and Technology.

Yutao XING received the B.S. degree from the School of Electronic and Optical Engineering, at Huaiyin Institute of Technology in 2023. Since 2023, he has worked toward the M.S. degree at Nanjing University of Science and Technology. His research interests include covert communications, deep learning, and UAV communication. His research interests include covert communications, deep learning, and UAV communication.